Expert Systems with Applications 38 (2011) 4058–4067

Contents lists available at ScienceDirect

Expert Systems with Applications

journal homepage: www.elsevier.com/locate/eswa

Feature extraction of forearm EMG signals for prosthetics

J. Rafiee [a,*], M.A. Rafiee [a], F. Yavari [a], M.P. Schoen [b]

[a] Department of Mechanical, Aerospace and Nuclear Engineering, JEC, 110 8th Street, Rensselaer Polytechnic Institute, NY 12180-3590, USA
[b] Measurement and Control Engineering Research Center, College of Engineering, Idaho State University, Pocatello, ID, USA

ARTICLE INFO

Keywords:
Prosthetics
Robotic hand
EMG
Signal classification
Feature extraction
Signal processing
Mother wavelet

ABSTRACT

This paper presents a new technique for feature extraction of forearm electromyographic (EMG) signals using a proposed mother wavelet matrix (MWM). A MWM including 45 potential mother wavelets is suggested to help the classification of surface and intramuscular EMG signals recorded from multiple locations on the upper forearm for ten hand motions. Also, a surface electrode matrix (SEM) and a needle electrode matrix (NEM) are suggested to select the proper sensors for each pair of motions. For this purpose, EMG signals were recorded from sixteen locations on the forearms of six subjects in ten hand motion classes. The main goal in classification is to define a proper feature vector able to generate acceptable differences among the classes. The MWM includes the mother wavelets which make the highest difference between two particular classes.

Six statistical feature vectors were compared using the continuous form of wavelet packet transform. The mother wavelet functions are selected with the aim of optimum classification between two classes using one of the feature vectors. The locations where the satisfactory signals are captured are selected from several mounted electrodes. Finally, three ten-by-ten symmetric MWM, SEM, and NEM represent the proper mother wavelet function and the surface and intramuscular selection for recording the ten hand motions.

Published by Elsevier Ltd.

1. Introduction

Classification and identification of biosignals (e.g. electromyographic (EMG) (e.g. Farina, Merletti, & Enoka, 2004; Merletti & Lo Conte, 1997; Rasheed, Stashuk, & Kamel, 2008) is still a challenge in several areas. EMG signals are complex due to the non-stationary characteristics and subject dependency of the signals (Aschero & Gizdulich, 2009). EMG signals are generally divided into two main groups: surface and needle EMG signals. Surface EMG signals have attracted remarkable attention in the design and manufacturing of artificial limbs (e.g. Fukuda, Tsuji, Kaneko, & Otsuka, 2003; Silvestro Micera, Sabatini, Dario, & Rossi, 1999). EMG classification is a complicated task since several parameters may effect the EMG signals, e.g. motor unit action potential (MUAP) (e.g. Kallenberg, Preece, Nester, & Hermens, 2009), muscle fatigue (e.g. Vukova, Vydevska-Chichova, & Radicheva, 2008), and force (Clancy, Bertolina, Merletti, & Farina, 2008). Two difficulties in EMG signal classification for prosthetic applications are the selection of electrode locations on the forearm and the extraction of a feature vector able to classify several motions, since the EMG signals are subject dependent. This research addresses these challenges in forearm EMG signals, which is applicable to the manufacturing of prosthetic hands. However, this research would not be able to address the other significant parameters, such as force, fatigue, and so forth for this application (e.g. Disselhorst-Klug, Schmitz-Rode, & Rau, 2009; Koike & Kawato, 1995; Liu, Herzog, & Savelberg, 1999).

To name a few examples of prior research, Park & Lee (1998) presented a fuzzy-based decision-making system to classify six motions of the six subjects, including elbow flexion and extension, wrist pronation and supination, and in and out humeral rotation. Englehart, Hudgins, Parker, & Stevenson (1999) compared frequency domain and time–frequency methods to preprocess EMG signals and introduced wavelet packet transform with satisfactory results. Englehart, Hudgins, & Parker (2001) applied the combination of wavelet packet and principal component analysis to extract suitable features from myoelectric signals to classify six classes of hand motions. Englehart & Hudgins (2003) also developed a wavelet-based system to control myoelectric signals of four classes of hand motions with high accuracy, low response time, and a user interface control system in 2003. Lowery, Stoykov, Taflove, & Kuiken (2002) presented a finite element method (FEM) model to investigate the effect of skin, muscle, fat, and bone tissue on simulated surface electromyographic (EMG) signals and demonstrated that all aforementioned materials have an effect on EMG signals. Gazzoni, Farina, & Merletti (2004) proposed an ANN-based automatic detection and identification system to pinpoint motor unit action potentials using wavelet transform and artificial neural

* Corresponding author. Tel.: +1 518 276 6351; fax: +1 518 276 6025.
E-mail addresses: rafiee@rpi.edu, krafiee81@gmail.com (J. Rafiee).

0957-4174/$ - see front matter Published by Elsevier Ltd.
doi:10.1016/j.eswa.2010.09.068

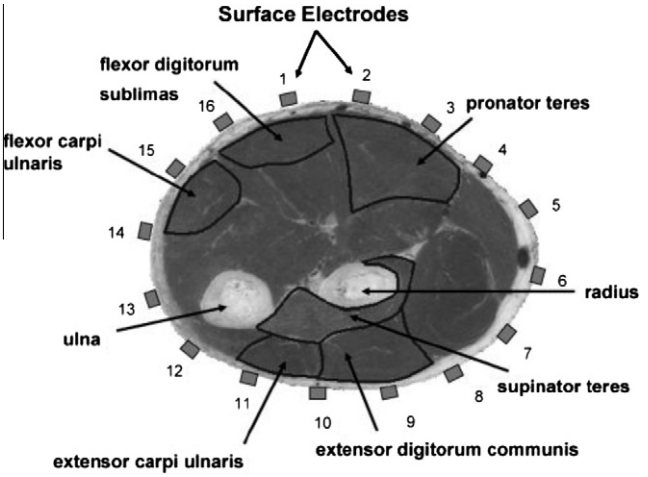

Fig. 1. A cross section of the upper forearm to illustrate the locations of 16 surface electrodes and six needle electrodes (Hargrove et al., 2007, with permission).

network in specific case studies. Sebelius et al. (2005) introduced an ANN-based intelligent system to classify seven hand movements for limited subjects.

In this research, a statistical-based feature extraction system is presented for nine hand motions plus a rest state, including key grip and chuck grip, two motions known for their difficulty in classification.

2. Surface and intramuscular EMG signals

In this research, both measures of forearm EMG signals have been collected and processed, although the major goal is surface EMG signal analysis, which is applicable to prosthetics. The experimental surface and intramuscular EMG signals used in this research have been provided by the Institute of Biomedical Engineering at the University of New Brunswick with a protocol approved by the University's Research Ethics Board (Hargrove, Englehart, & Hudgins, 2007). Two different data acquisition systems were used to collect surface and intramuscular EMG signals (Hermens et al., 1999). For surface EMG signals, a 16-electrode linear array with interelectrode spacing of 2 cm was used (see Fig. 1). Each channel was filtered between 10 and 500 Hz and amplified with a gain of two thousand. Frequency information of surface EMG is shown in Fig. 2 for one subject using power spectrum density (PSD). For intramuscular EMG, needles were implanted in the pronator and supinator teres, flexor digitorum sublimas, extensor digitorum communis, and flexor and extensor carpi ulnaris. These measures were used to record time-domain signals regarding grip, wrist flexion and rotation, and gross movement. These six channels of data were also filtered and amplified (see Fig. 1). These were recorded in six subjects while they performed the ten hand movements for 5 s each, with a 2 min resting period after each exercise. The tests were repeated for each subject, resulting in 10 s of EMG signals per person for each motion. The subjects denied feeling fatigued during these exercises. The studied hand motions includes forearm pronation (FP), forearm supination (FS), wrist flexion (WF), wrist extension (WE), wrist abduction (WAB), wrist adduction (WAD), key grip (KG), chuck grip (CG), spread fingers (SF), and a rest state (RS).

3. Wavelet transform

Wavelet transform is being used in broad areas of biosignal processing (e.g. Beck et al., 2005; Cvetkovic, Übeyli, & Cosic, 2008; Hostens, Seghers, Spaepen, & Ramon, 2004; Kurt, Sezgin, Akin, Kirbas, & Bayram, 2009; Rafiee, Rafiee, Prause, & Schoen, 2009; Subasi, 2005; Tscharner, 2008; von Tscharner, 2000; Rafiee, Rafiee, & Michaelsen, 2009). Wavelet transform (Daubechies, 1991) is generally divided into either a discrete and or continuous form (Unser & Aldroubi, 1996). The continuous wavelet transform (CWT) of a signal $s(t)$ is defined as the integral of the product between the signal $s(t)$ and the daughter wavelets, which are the time translation and scale expansion/compression versions of a mother wavelet function $\psi(t)$. Equivalent to a scalar production, this calculation generates continuous wavelet coefficients CWC (a,b), which

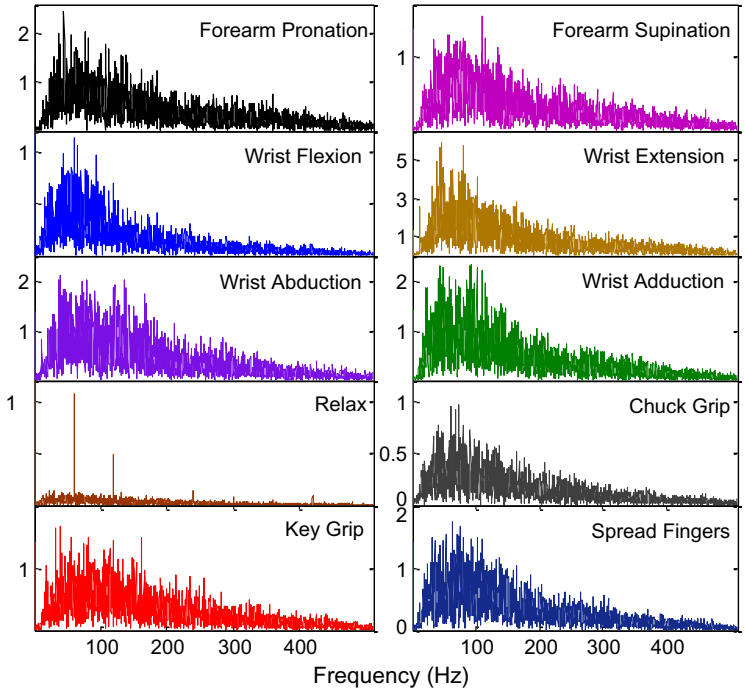

Fig. 2. Power spectrum density (PSD) of surface EMG signals of ten hand motions recorded from one of the 16 channels of the data acquisition system.

determine the similarity between the signal and the daughter wavelets located at position b (time shifting factor) and positive scale a:

$$\mathrm{CWC}(a,b) = \int_{-\infty}^{+\infty} s(t)\frac{1}{\sqrt{a}}\psi^*\left(\frac{t-b}{a}\right)dt, \quad (1)$$

where * stands for complex conjugation and $\psi \in L^2(R)\backslash\{0\}$. In the frequency domain, Eq. (1) is expressed as:

$$F\{\mathrm{CWC}(a,b)\} = \sqrt{a}\Psi^*(a.\omega)S(\omega), \quad (2)$$

where $F\{\mathrm{CWC}(a,b)\}$, $\Psi^*(\omega)$, and $S(\omega)$ stand for the Fourier transforms of the continuous wavelet coefficients CWC (a,b), the signal $s(t)$, and the mother wavelet function ψ (t), respectively. Eq. (2) shows that a mother wavelet function is a band-pass filter in the frequency domain, and the use of CWC identifies the local features of the signal. According to the theory of Fourier transform, the center frequency of the mother wavelet Ψ $(a\omega)$ is defined asF_0/a, given that the center frequency of the $\Psi(\omega)$ is F_0. Consequently, extraction of frequency contents from the signal is possible in different scales. In the windowed Fourier transform, the frequency resolution is constant and depends on the width of window. However, wavelet transform offers a rich analysis for a wide variety of window widths as the function of a. Use of a wide variety of mother wavelet functions, which must satisfy the admissibility condition C_ψ, is another advantage of wavelet analysis:

$$C_\psi = \int_{-\infty}^{+\infty} \frac{|\Psi(\omega)|^2}{\omega} d\omega \prec \infty. \quad (3)$$

C_ψ is satisfied if the mean value of the mother wavelet function $\psi(t)$ is equal to zero and $\psi(t)$ decays to zero rapidly when $t \to \pm\infty$. If the mother wavelet satisfies the above condition as well as orthogonality, the signal can be reconstructed from wavelet coefficients.

Unlike DWT, CWT operates at any scale and is continuous in terms of shifting. In the calculation of CWC, the mother wavelet is shifted smoothly throughout the analyzed signal/function and gives rich time–frequency information. The main drawback of CWT is that the computation is time-consuming. For signals with low signal to noise ratio, CWT could work better than DWT because DWT down-sampling of the signals can lead to the loss of significant information. Wavelet decomposition of the signals is also divided into two main branches: pyramid and packet decompositions. In both methods, signals are divided into approximation (low frequencies) and detail (high frequencies) in the first level. In the pyramid decomposition, after the first level, only approximations are permitted to be decomposed through higher levels. However, in the packet decomposition both approximation and detail are decomposed into further levels. Therefore, packet decomposition offers rich contents of signals. For EMG signals, the significant frequency contents are achieved in high scales. Continuous wavelet transform, which means continuous shifting

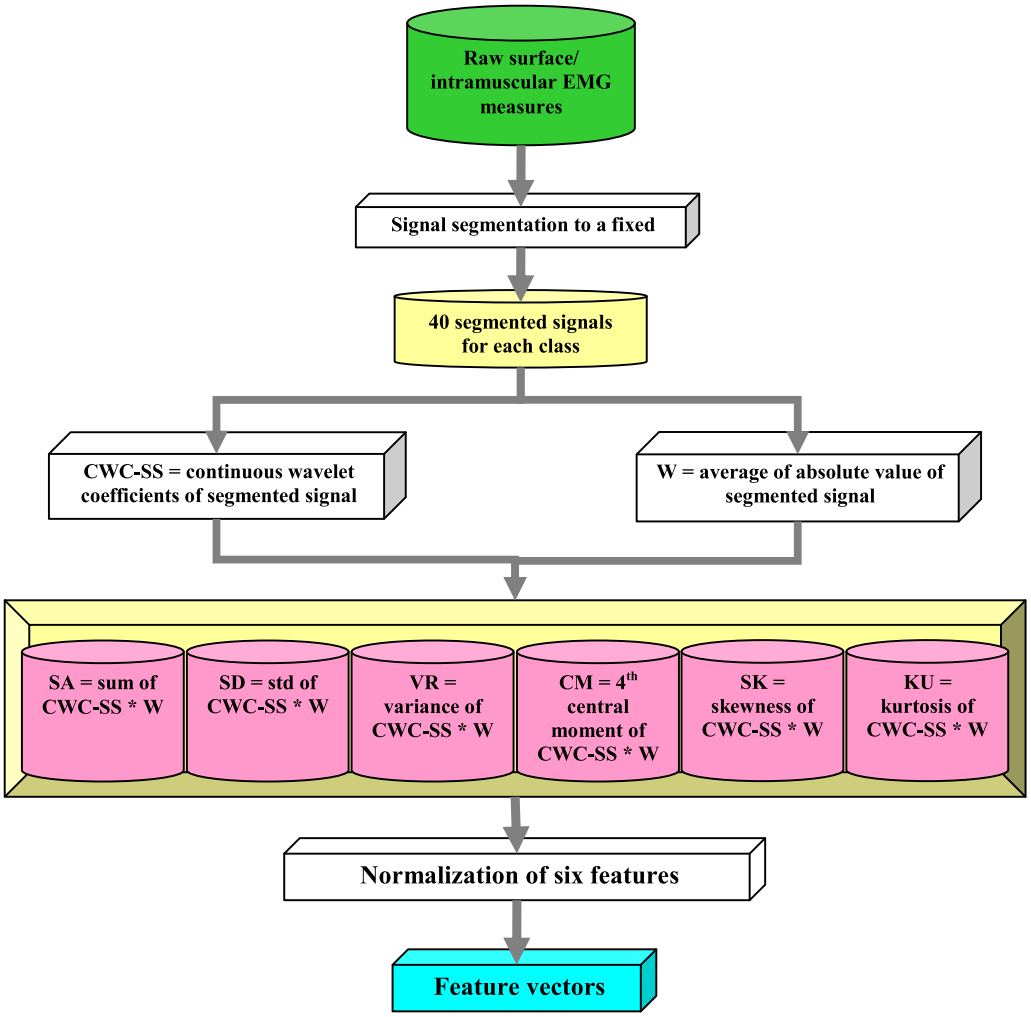

Fig. 3. Feature extraction algorithm.

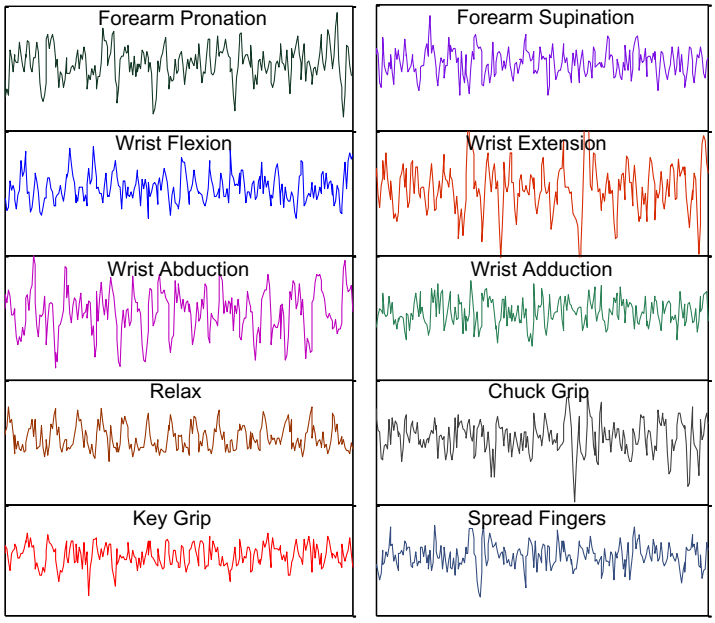

Fig. 4. Segmented surface EMG in a 256-points window from one subject performing 10 hand motions.

through time, is used with packet decomposition in this research. Therefore, CWT converts a one-dimensional signal $s(t)$ into a matrix of CWC (a,b) as follows:

$$\mathrm{CWC}(a,b) = \frac{T_s}{\sqrt{|a|}} \sum_{n=0}^{N-1} \psi^* \left[\frac{(n-i)T_s}{a} \right] s(nT_s), \tag{4}$$

where $i = 0,1,2,\ldots,N$, T_s and N stand for sampling time and the number of samples, respectively.

In classification, feature vector is defined as a compressed, meaningful vector/matrix possessing the significant information of different classes. In this research, CWC is used for the calculation of feature vectors for EMG signals. The CWC of the signal, itself, is not appropriate as a feature vector because it is computationally expensive. Hence, further processing is needed in order to define a precise and compressed feature vector, which is explained in the next section.

4. Mother wavelet matrix and sensor selection

Selection of the mother wavelet function, a challenge in wavelet transform, was studied in this research by introducing MWM. Prior contributions on mother wavelet functions can be found in literature (e.g. Brechet, Lucas, Doncarli, & Farina, 2007; Farina, do Nascimento, Lucas, & Doncarli, 2007, 2008; Lucas, Gaufriau, Pascual, Doncarli, & Farina, 2008; Rafiee & Tse, 2009).

Two points regarding the application of mother functions are discussed here. The first concern is the selection of proper mother wavelet function since the application of mother wavelets is problem-dependent. Applicable mother wavelet functions in EMG signal processing could vary depending on the parameters of the problem at hand. If the technique is based on the similarity of the signal to the mother function, then the most important factor is the amplitude of the wavelet coefficient across the signals. The mother functions similar to the signal are not suitable for all wavelet-based approaches. A clear example is the wide application of

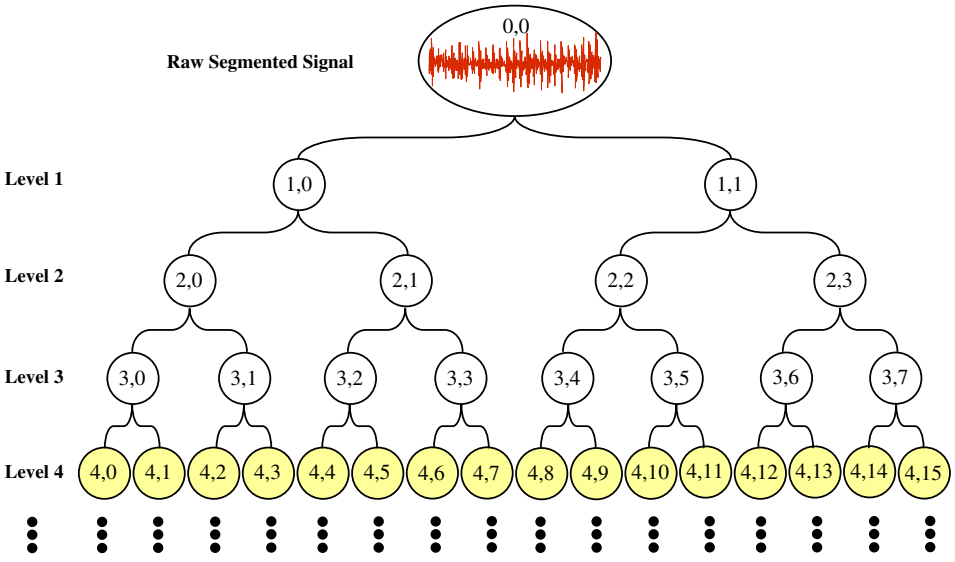

Fig. 5. Decomposition tree and the level of decomposition.

the Haar function, which is dissimilar to the signals but has been introduced as a relatively efficient function in several studies (Subramani, Sahu, & Verma, 2006). In wavelet-based classification systems the mother wavelet functions are related to the problem parameters rather than the shape of signals, unless the method was established based on signal similarity. Another issue in EMG signal classification is the optimal sensor selection. Applicable sensor selection depends on the problem as well. For example, optimal selection of sensors for prosthetic hands to classify six motions is different from those for eight motions. To reduce the computational time for real-time control of a prosthetic hand, the optimal electrodes to be chosen are presented for the ten motions classification by introducing surface electrode matrix (SEM) and needle electrode matrix (NEM) in this research.

First, the feature vector is defined based on the following steps (see flowchart in Fig. 3):

1. Signal segmentation: in this research, surface and intramuscular EMG signals were separately classified for ten hand motions, although intramuscular EMG signals may not be applicable to prosthetics. However, comparisons between surface EMG classification and intramuscular EMG classification may be helpful. After recording EMG signals by means of sixteen electrodes for surface and six electrodes for intramuscular EMG, the raw signals were segmented into the 256-point windows (Hargrove et al., 2007) as shown in Fig. 4 for surface EMG signals. For simplicity, a signal with a length of 256 points is called the segmented signal. Therefore, a matrix of segmented signals (a 16×256 matrix for surface and a 6×256 matrix for intramuscular EMG) can be one input for the control system of prosthetic hand. As mentioned, recorded EMG signals of six subjects were studied. For all ten motions, surface and intramuscular EMG signals were recorded in two separate 5-s exercises for each of six subjects (40 segmented signals for each subject/each hand motion were obtained).
2. In the fourth decomposition level (see Fig. 5), continuous wavelet coefficients of the segmented signals (CWC-SS) were calculated (2^4scales for each segmented unit signal).
3. The average of the absolute value of the segmented signals (1×256 vector) were calculated for each segmented signal and titled 'weight' (W) to construct the feature vector as follows:

$$W = \frac{1}{N}\sum_{i=1}^{N}|s_i(t)|, \tag{5}$$

where N is the number of datapoints in each segmented signal (256 in this research).

4. The calculation of feature vectors – six feature vectors are studied in this research:

($\surd$) Weighted sum of absolute value of CWC-SS (SA) is calculated as the sum of the absolute value of CWC-SS multiplied by the average of the absolute value of the segmented signals (weight).

$$SA(a_{15}, b) = W\left(\sum_{n=1}^{N}|\mathrm{CWC}(a_{15}, b)|\right), \tag{6}$$

where a_{15} is the scale related to (4, 15) in the decomposition tree (see Fig. 5). Scale selection is another important issue in wavelet analysis. Decomposing the signals into higher scales leads to a greater focus on the frequency domain (Rafiee & Tse, 2009). Nevertheless, computational time in CWT is of paramount significance, and going through high scales makes the computations for the real-time control system of the prosthetic hand difficult. In this research, the fourth level of decomposition has been considered the reasonable level. Based on trial-and-error, a_{15} represented larger wavelet coefficients, and subsequently the daughter wavelet at this scale is more similar to both classes of EMG signals, which, at that scale, leads to a greater difference in the wavelet coefficient from one motion to another.

($\surd$) Weighted standard deviation of CWC-SS (SD) is calculated as the standard deviation of CWC-SS multiplied by the average of the absolute value of the segmented signals (weight).

$$SD(a_{15}, b) = W\left(\sqrt{\frac{1}{N-1}\sum_{n=1}^{N}(CWC_n(a_{15}, b) - \overline{\mathrm{CWC}(a_{15}, b)})^2}\right), \tag{7}$$

where:

$$\overline{\mathrm{CWC}(a_{15}, b)} = \frac{1}{N}\left(\sum_{n=1}^{N}CWC_n(a_{15}, b)\right). \tag{8}$$

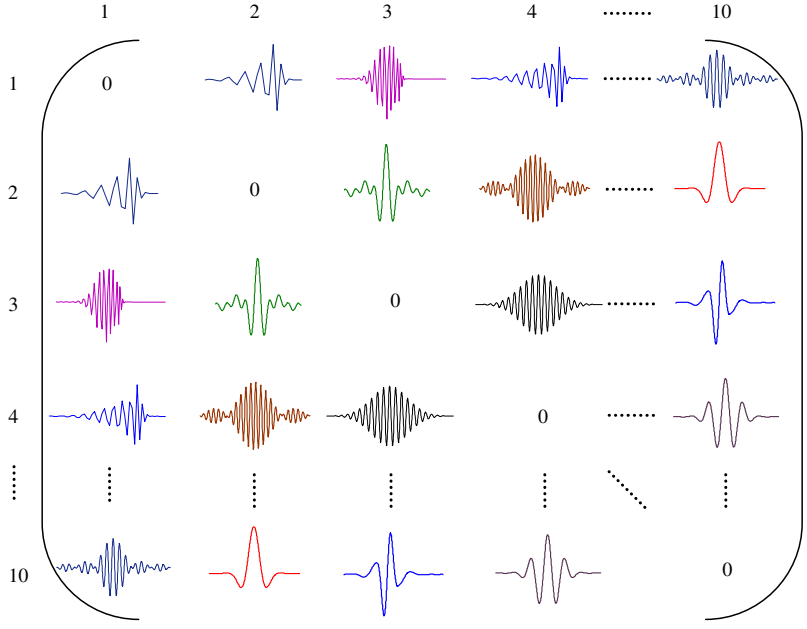

Fig. 6. Schematic of mother wavelet matrix (MWM) (Rafiee et al., 2009).

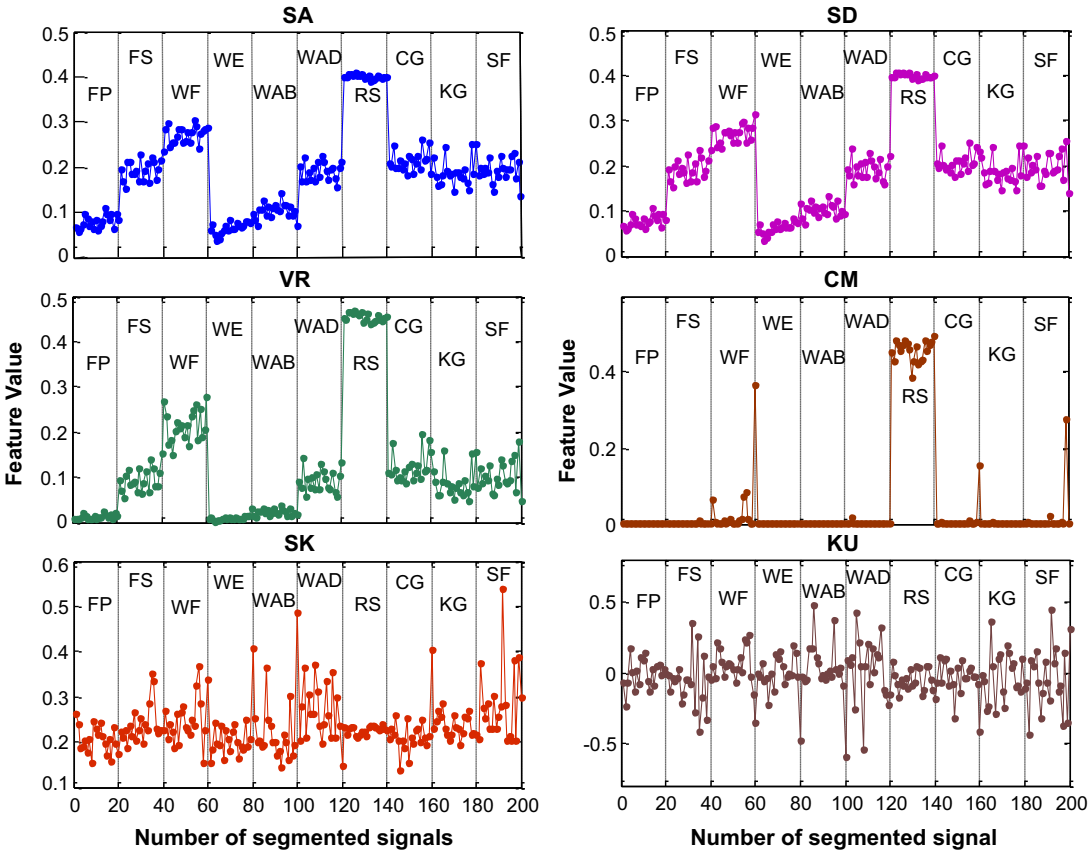

Fig. 7a. Extracted features from surface EMG of one specific subject (sensor 13, scale (4,15).

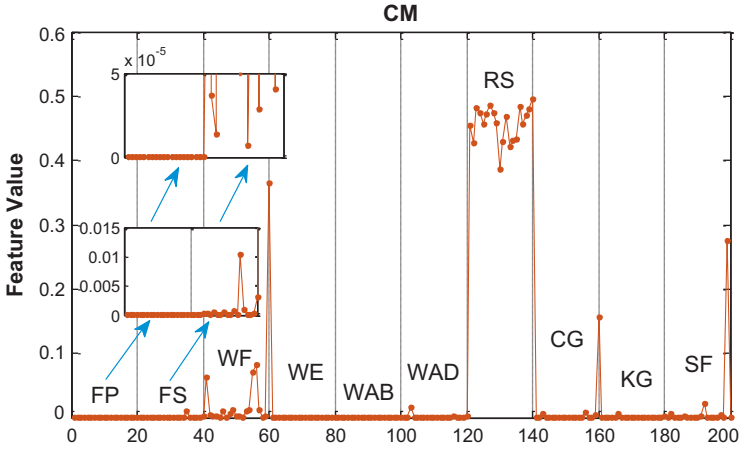

Fig. 7b. CM feature extracted from surface EMG of one specific subject (sensor 13, scale (4,15).

0	shan 2-0.8	bior3.1	shan 2-0.9	cmor3-0.2	bior3.1	cmor1-0.3	cmor1-0.3	shan 2-0.8	shan 2-0.9
	0	cmor1-1.5	cmor1-0.5	shan 0.5-0.1	shan 0.5-0.1	shan 0.5-0.1	shan 0.5-0.1	shan 0.5-0.1	shan 0.2-0.1
		0	cmor1-0.5	shan 0.2-0.1	shan 0.2-0.1	shan 0.2-0.1	shan 0.2-0.1	shan 0.2-0.1	shan 0.2-0.1
			0	bior3.1	bior3.1	shan 0.5-0.1	shan 0.5-0.1	bior3.1	bior3.1
				0	bior3.1	shan 0.5-0.1	shan 0.5-0.1	shan 0.5-0.1	shan 0.5-0.1
					0	shan 0.2-0.1	shan 0.2-0.1	shan 0.2-0.1	shan 0.2-0.1
						0	cmor1-1.5	rbio3.1	rbio2.6
							0	cmor4-0.1	shan 1-0.9
								0	shan 2-0.5
									0

Fig. 8a. Mother wavelet matrix for surface EMG signals.

0	cmor3-0.3	shan2-0.9	cmor1-0.05	cmor2-0.3	bior3.1	shan2-0.5	shan2-0.5	cmor4-0.2	shan2-0.5
	0	cmor4-0.2	shan2-0.5	cmor1-1.5	fbsp2-0.2-0.1	shan0.5-0.2	shan1-0.2	shan2-0.7	shan1-0.3
		0	'shan1-0.2	cmor1-1.5	shan1-0.2	cmor3-0.2	bior3.1	shan2-0.9	shan1-0.2
			0	bior3.1	bior3.1	shan0.2-0.1	shan0.2-0.1	shan2-0.9	shan0.2-0.1
				0	cmor2-2.6	shan1-0.2	shan0.5-0.1	shan2-0.6	shan1-0.2
					0	shan0.5-0.1	bior3.1	shan1-0.1	shan0.5-0.1
						0	cmor2-2.3	cmor3-0.3	cmor2-2.1
							0	shan0.5-0.1	bior3.1
								0	cmor2-2.2
									0

Fig. 8b. Mother wavelet matrix for intramuscular EMG signals.

- √ Weighted variance of CWC-SS (VR) is calculated as the variance of CWC-SS multiplied by weight, as the last steps for SD and SA are defined.
- √ Weighted fourth central moment of CWC-SS (CM) is calculated as the fourth central moment of CWC-SS multiplied by weight. The basic formula is not included for simplicity.
- √ Weighted skewness of CWC-SS (SK) is calculated as the skewness of CWC-SS multiplied by weight.
- √ Weighted kurtosis of CWC-SS (KU) is calculated as the kurtosis of CWC-SS multiplied by weight.

5. All these features are normalized to make the calculations consistent. SA feature was one of the features showing better classification performance for both surface and intramuscular EMG signals comparing to the others. Therefore, SA was considered the main feature to define the mother wavelet matrix. Schematic of MWM is shown in Fig. 6. In this figure, the horizontal/vertical numbers (1,2,...,10) corresponds to the motions: forearm pronation, forearm supination, wrist flexion, wrist extension, wrist abduction, wrist adduction, rest state, chuck grip, key grip and spread fingers, respectfully.

After selection of the feature, the following procedure is applied to find the MWM, SEM, and NEM:

For each pair of motions the corresponding entity of MWM matrix is the function ψ that possesses the minimum value for the criterion, $C(\psi)$:

$$\forall i,j=1,\ldots,10 \text{ and } i\neq j MWM(i,j)=\psi:\min_{\psi}\left(C(\psi)=\frac{1}{L}\sum_{l=1}^{L}D_l(\psi)\right), \tag{9}$$

where L is the number of the electrodes, and ψ is selected from a pool of 324 wavelet basis function (see Tables 1A and 1B)

$$D_l(\psi)=\frac{R_i(\psi)+R_j(\psi)}{|M_i(\psi)-M_j(\psi)|}, \tag{10}$$

where $R_i(\psi)$ is the range of SA function for all $k = 1,\ldots,N = 240$ segmented signals for ith motion ($N = 240$ since there are six subjects and 40 segmented signals for each subject):

$$R_i(\psi)=|\min_k(SA_{ik}(\psi))-\max_k(SA_{ik}(\psi))|. \tag{11}$$

In Eq. (10), $M_i(\psi)$ is the average value of SA function for all $k = 1,\ldots,N$ segmented signals for ith motion:

$$M_i(\psi)=\frac{1}{K}\sum_{k=1}^{N}SA_{ik}(\psi), \tag{12}$$

where $SA_{ik}(\psi)$ is the value of SA function for ith motion and kth segmented signal calculated by Eq. (6).

By minimizing the value of $C(\psi)$ and therefore the value of $D_l(\psi)$ for each pair of motions, the mother wavelet having the less range of feature values for N segmented signals and more difference between two motions is selected.

The same procedure is considered to calculate MWM for intramuscular EMG signals. After finding MWM matrix, NEM and SEM matrices can be obtained. For each pair of motions, the corresponding entity of SEM matrix is the surface electrode number (see Fig. 1), which has the minimum value of $D_l(\psi)$ function (Eq. 10) calculated for corresponding mother wavelet extracted from MWM matrix. The same procedure is repeated for EMG intramuscular signals ending up with NEM matrix.

5. Results and discussion

In this research, six statistical features are studied for surface and intramuscular EMG signals as shown in Fig. 7a for one specific scale recorded from a specific sensor attached to the arm of one subject. Among the features, SK and KU did not show proper classification for this scale/sensor and neither for the others

$$SEM=\begin{array}{c} \\ 1\\2\\3\\4\\5\\6\\7\\8\\9\\10\end{array}\begin{array}{c}\begin{array}{cccccccccc}1&2&3&4&5&6&7&8&9&10\end{array}\\\begin{bmatrix}0&13&15&9&9&5&13&13&6&13\\&0&13&1&12&5&15&9&7&13\\&&0&3&9&8&13&9&7&8\\&&&0&13&15&3&15&6&15\\&&&&0&15&2&2&6&6\\&&&&&0&4&9&4&13\\&&&&&&0&9&6&8\\&&&&&&&0&6&15\\&&&&&&&&0&3\\&&&&&&&&&0\end{bmatrix}\end{array}$$

Fig. 9a. Selected sensors within surface electrode matrix (SEM).

$$NEM=\begin{array}{c} \\ 1\\2\\3\\4\\5\\6\\7\\8\\9\\10\end{array}\begin{array}{c}\begin{array}{cccccccccc}1&2&3&4&5&6&7&8&9&10\end{array}\\\begin{bmatrix}0&4&4&2&4&6&5&5&6&5\\&0&2&2&1&2&6&3&6&5\\&&0&2&1&2&3&1&4&2\\&&&0&5&6&5&5&6&5\\&&&&0&6&6&5&4&6\\&&&&&0&5&1&5&5\\&&&&&&0&3&4&3\\&&&&&&&0&6&3\\&&&&&&&&0&1\\&&&&&&&&&0\end{bmatrix}\end{array}$$

Fig. 9b. Selected intramuscular sensors within needle electrode matrix (NEM).

Table 1A
Studied wavelet families in this research.

No.	Family (short form)	Order
1	Haar (db1)	db 1
2–45	Daubechies (db)	db 2–db 45
46–50	Coiflet (coif)	coif 1–coif 5
51	Morlet (Morl)	morl
52–147	Complex Morlet (cmor Fb–Fc)[a]	Included Table 1B
148	Discrete Meyer (dmey)	dmey
149	Meyer (meyr)	meyr
150	Mexican Hat (mexh)	mexh
151–200	Shannon (Shan Fb–Fc)[a]	Included Table 1B
201–260	Frequency B-Spline (fbsp M–Fb–Fc)[a]	Included Table 1B
261–267	Gaussian (gaus)	gaus 1 to gaus7
268–275	Complex Gaussian (cgau)	cgau 1 to cgau8
276–290	Biorthogonal (bior Nr.Nd)[b]	Included Table 1B
291–305	Reverse biorthogonal (rbio Nr.Nd)[b]	Included Table 1B
306–324	Symlet (sym)	sym 2 to sym 20

[a] Fb is a bandwidth parameter, Fc is a wavelet center frequency, *M* is an integer order parameter.
[b] Nr and Nd are orders: *r* for reconstruction/d for decomposition.

(see Fig. 7a). The other four features can be useful for forearm EMG signal classification. It is worth mentioning that CM feature shown in Fig. 7a cannot visually show proper classification. However, by zooming on the CM plot, more information may be observed as plotted in Fig. 7b.

Also, mother wavelet matrices (MWM) matched with our experimental data is shown in Figs. 8a and 8b for surface and intramuscular EMG signals respectfully (see Appendix A, for function detail). As it can be seen from the matrix in Fig. 8a, NEM and SEM have been also depicted in Figs. 9a and 9b for surface EMG dataset used in this research for validation. The numbers in these matrices are referred to the sensor number shown in Fig. 1. As it can be seen in NEM and SEM, sensor number 9, located close to extensor digitorum communis, number 13, located in between extensor and flexor carpi ulnaris, and number 15, close to flexor carpi ulnaris offer more helpful information for feature extraction of the above mentioned ten motions.

The advantages of the proposed technique can be summarized as follows:

Table 1B
Studied wavelet families in detail.

No	Wave	No	Wave	No	Wave	No	Wave	No	Wave
52	1–1.5	100	3–1.1	148	dmey	196	2–0.6	244	2–0.2–0.4
53	1–1	101	3–1.2	149	meyr	197	2–0.7	245	2–0.2–0.5
54	1–0.5	102	3–1.3	150	mexh	198	2–0.8	246	2–0.2–0.6
55	1–0.3	103	3–1.4	151	0.1–0.1	199	2–0.9	247	2–0.2–0.7
56	1–0.2	104	3–1.5	152	0.1–0.2	200	1–1	248	2–0.2–0.8
57	1–0.1	105	3–1.6	153	0.1–0.3	201	1–0.1–0.1	249	2–0.2–0.9
58	1–0.05	106	3–1.8	154	0.1–0.4	202	1–0.1–0.2	250	2–0.2–1
59	1–0.02	107	3–1.9	155	0.1–0.5	203	1–0.1–0.3	251	3–0.2–0.1
60	1–0.01	108	3–2	156	0.1–0.6	204	1–0.1–0.4	252	3–0.2–0.2
61	2–0.1	109	3–2.1	157	0.1–0.7	205	1–0.1–0.5	253	3–0.2–0.3
62	2–0.2	110	3–2.2	158	0.1–0.8	206	1–0.1–0.6	254	3–0.2–0.4
63	2–0.3	111	3–2.3	159	0.1–0.9	207	1–0.1–0.7	255	3–0.2–0.5
64	2–0.4	112	3–2.4	160	0.1–1	208	1–0.1–0.8	256	3–0.2–0.6
65	2–0.5	113	3–2.5	161	0.2–0.1	209	1–0.1–0.9	257	3–0.2–0.7
66	2–0.6	114	3–2.6	162	0.2–0.2	210	1–0.1–1	258	3–0.2–0.8
67	2–0.7	115	3–2.7	163	0.2–0.3	211	2–0.1–0.1	259	3–0.2–0.9
68	2–0.8	116	3–2.8	164	0.2–0.4	212	2–0.1–0.2	260	3–0.2–1
69	2–0.9	117	3–2.9	165	0.2–0.5	213	2–0.1–0.3	276	1.1
70	2–1	118	3–3	166	0.2–0.6	214	2–0.1–0.4	277	1.3
71	2–1.1	119	4–0.1	167	0.2–0.7	215	2–0.1–0.5	278	1.5
72	2–1.2	120	4–0.2	168	0.2–0.8	216	2–0.1–0.6	279	2.2
73	2–1.3	121	4–0.3	169	0.2–0.9	217	2–0.1–0.7	280	2.4
74	2–1.4	122	4–0.4	170	0.2–1	218	2–0.1–0.8	281	2.6
75	2–1.5	123	4–0.5	171	0.5–0.1	219	2–0.1–0.9	282	2.8
76	2–1.6	124	4–0.6	172	0.5–0.2	220	2–0.1–1	283	3.1
77	2–1.8	125	4–0.7	173	0.5–0.3	221	3–0.1–0.1	284	3.3
78	2–1.9	126	4–0.8	174	0.5–0.4	222	3–0.1–0.2	285	3.5
79	2–2	127	4–0.9	175	0.5–0.5	223	3–0.1–0.3	286	3.7
80	2–2.1	128	4–1	176	0.5–0.6	224	3–0.1–0.4	287	3.9
81	2–2.2	129	4–1.1	177	0.5–0.7	225	3–0.1–0.5	288	4.4
82	2–2.3	130	4–1.2	178	0.5–0.8	226	3–0.1–0.6	289	5.5
83	2–2.4	131	4–1.3	179	0.5–0.9	227	3–0.1–0.7	290	6.8
84	2–2.5	132	4–1.4	180	0.5–1	228	3–0.1–0.8	291	1.1
85	2–2.6	133	4–1.5	181	1–0.1	229	3–0.1–0.9	292	1.3
86	2–2.7	134	4–1.6	182	1–0.2	230	3–0.1–1	293	1.5
87	2–2.8	135	4–1.8	183	1–0.3	231	1–0.2–0.1	294	2.2
88	2–2.9	136	4–1.9	184	1–0.4	232	1–0.2–0.2	295	2.4
89	2–3	137	4–2	185	1–0.5	233	1–0.2–0.3	296	2.6
90	3–0.1	138	4–2.1	186	1–0.6	234	1–0.2–0.4	297	2.8
91	3–0.2	139	4–2.2	187	1–0.7	235	1–0.2–0.5	298	3.1
92	3–0.3	140	4–2.3	188	1–0.8	236	1–0.2–0.6	299	3.3
93	3–0.4	141	4–2.4	189	1–0.9	237	1–0.2–0.7	300	3.5
94	3–0.5	142	4–2.5	190	1–1	238	1–0.2–0.8	301	3.7
95	3–0.6	143	4–2.6	191	2–0.1	239	1–0.2–0.9	302	3.9
96	3–0.7	144	4–2.7	192	2–0.2	240	1–0.2–1	303	4.4
97	3–0.8	145	4–2.8	193	2–0.3	241	2–0.2–0.1	304	5.5
98	3–0.9	146	4–2.9	194	2–0.4	242	2–0.2–0.2	305	6.8
99	3–1	147	4–3	195	2–0.5	243	2–0.2–0.3		

1. The number of motions was increased to ten hand motions. Chuck and key grips, which are the complicated motions for classification because of the engagements of several in-depth muscles and complexity of the signals, were studied by the proposed algorithm.
2. The presented features would also be appropriate for training purposes of intelligent classifiers (e.g. Micera, Sabatini, & Dario, 2000; Pandey & Mishra, 2009; Rafiee et al., 2009; Xie, Zheng, Guo, Chen, & Shi, 2009) or to determine rules for fuzzy systems (Chan, Yang, Lam, Zhang, & Parker, 2000).
3. This method was able to find optimal sensors for each pair of motions applicable for classification purposes.

6. Conclusions

A method was suggested to extract appropriate features for forearm electromyographic (EMG) signals using a mother wavelet matrix (MWM). After broad investigations on 324 mother wavelet functions, the combination of some mother wavelets ameliorated the EMG signal analysis. Among several installed electrodes on the subjects' forearms, the optimal sensors appropriate for feature extraction were selected in terms of surface electrode matrix (SEM) and a needle electrode matrix (NEM). Six statistical feature vectors were also studied in this research.

Acknowledgments

The authors would like to offer special thanks to Professor Kevin Englehart, associate director of the Institute of Biomedical Engineering at University of New Brunswick, who supported us with experimental EMG signals used in this research. The authors also acknowledges funding support from the US DARPA (Award Number: W81XWH-07-2-0078) for Idaho State University Smart Prosthetic Hand Technology – Phase I.

Appendix A

Tables 1A, 1B.

References

Aschero, G., & Gizdulich, P. (2009). Denoising of surface EMG with a modified Wiener filtering approach. *Journal of Electromyography and Kinesiology*. doi:10.1016/j.jelekin.2009.02.003.

Beck, T. W., Housh, T. J., Johnson, G. O., Weir, J. P., Cramer, J. T., Coburn, J. W., et al. (2005). Comparison of Fourier and wavelet transform procedures for examining mechanomyographic and electromyographic frequency versus isokinetic torque relationships. *Electromyography and Clinical Neurophysiology, 45*(2), 93–103.

Brechet, L., Lucas, M. F., Doncarli, C., & Farina, D. (2007). Compression of biomedical signals with mother wavelet optimization and best-basis wavelet packet selection. *IEEE Transactions on Biomedical Engineering, 54*(12).

Chan, F. H. Y., Yang, Y.-S., Lam, F. K., Zhang, Y.-T., & Parker, P. A. (2000). Fuzzy EMG classification for prosthesis control. *IEEE Transactions on Rehabilitation Engineering, 8*(3), 305–311.

Clancy, E. A., Bertolina, M. V., Merletti, R., & Farina, D. (2008). Time- and frequency-domain monitoring of the myoelectric signal during a long-duration, cyclic, force-varying, fatiguing hand-grip task. *Journal of Electromyography and Kinesiology, 18*, 789–797.

Cvetkovic, D., UЁeyli, E. D., & Cosic, I. (2008). Wavelet transform feature extraction from human PPG, ECG, and EEG signal responses to ELF PEMF exposures: A pilot study. *Digital Signal Processing: A Review Journal, 18*(5), 861–874.

Daubechies, I. (1991). *Ten lectures on wavelets. CBMS-NSF series in applied mathematics*. Philadelphia, PA: SIAM.

Disselhorst-Klug, C., Schmitz-Rode, T., & Rau, G. (2009). Surface electromyography and muscle force: Limits in sEMG-force relationship and new approaches for applications. *Clinical Biomechanics, 24*(3), 225–235.

Englehart, K., & Hudgins, B. (2003). A robust, real-time control scheme for multifunction myoelectric control. *IEEE Transactions on Biomedical Engineering, 50*(7).

Englehart, K., Hudgins, B., & Parker, P. A. (2001). A wavelet-based continuous classification scheme for multifunction myoelectric control. *IEEE Transactions on Biomedical Engineering, 48*(3), 302–311.

Englehart, K., Hudgins, B., Parker, P. A., & Stevenson, M. (1999). Classification of the myoelectric signal using time–frequency based representations. *Medical Engineering and Physics, 21*, 431–438.

Farina, D., do Nascimento, O. F., Lucas, M. F., & Doncarli, C. (2007). Optimization of wavelets for classification of movement-related cortical potentials generated by variation of force-related parameters. *Journal of Neuroscience Methods, 162*, 357–363.

Farina, D., Lucas, M. F., & Doncarli, C. (2008). Optimized wavelets for blind separation of non-stationary surface myoelectric signals. *IEEE Transactions on Biomedical Engineering, 55*(1).

Farina, D., Merletti, R., & Enoka, R. M. (2004). The extraction of neural strategies from the surface EMG. *Journal of Applied Physiology, 96*(4), 1486–1495.

Fukuda, O., Tsuji, T., Kaneko, M., & Otsuka, A. (2003). A human-assisting manipulator teleoperated by EMG signals and arm motions. *IEEE Transactions on Robotics and Automation, 19*(2), 210–222.

Gazzoni, M., Farina, D., & Merletti, R. (2004). A new method for the extraction and classification of single motor unit action potentials from surface EMG signals. *Journal of Neuroscience Methods, 136*, 165–177.

Hargrove, L. J., Englehart, K., & Hudgins, B. (2007). A comparison of surface and intramuscular myoelectric signal classification. *IEEE Transactions on Biomedical Engineering, 54*(5).

Hermens, H., Freriks, B., Merletti, R., Stegeman, D., Blok, J., Rau, G., Disselhorst-Klug, C., et al. (1999). *European recommendations for surface electromyography*. RRD Publisher.

Hostens, I., Seghers, J., Spaepen, A., & Ramon, H. (2004). Validation of the wavelet spectral estimation technique in Biceps Brachii and Brachioradialis fatigue assessment during prolonged low-level static and dynamic contractions. *Journal of Electromyography and Kinesiology, 14*, 205–215.

Kallenberg, L. A. C., Preece, S., Nester, C., & Hermens, H. J. (2009). Reproducibility of MUAP properties in array surface EMG recordings of the upper trapezius and sternocleidomastoid muscle. *Journal of Electromyography and Kinesiology*. doi:10.1016/ j.jelekin. 2008.11.012.

Koike, Y., & Kawato, M. (1995). Estimation of dynamic joint torques and trajectory formation from surface electromyography signals using a neural network model. *Biological Cybernetics, 73*(4), 291–300.

Kurt, M. B., Sezgin, N., Akin, M., Kirbas, G., & Bayram, M. (2009). The ANN-based computing of drowsy level. *Expert Systems with Applications, 36*(2 part 1), 2534–2542.

Liu, M. M., Herzog, W., & Savelberg, H. H. C. M. (1999). Dynamic muscle force predictions from EMG: An artificial neural network approach. *Journal of Electromyography and Kinesiology, 9*(6), 391–400.

Lowery, M. M., Stoykov, N. S., Taflove, A., & Kuiken, T. A. (2002). A multiple-layer finite-element model of the surface EMG signal. *IEEE Transactions on Biomedical Engineering, 49*(5).

Lucas, M. F., Gaufriau, A., Pascual, S., Doncarli, C., & Farina, D. (2008). Multi-channel surface EMG classification using support vector machines and signal-based wavelet optimization. *Biomedical Signal Processing and Control*(3), 169–174.

Merletti, R., & Lo Conte, L. R. (1997). Surface EMG signal processing during isometric contractions. *Journal of Electromyography and Kinesiology, 7*(4), 241–250.

Micera, S., Sabatini, A. M., & Dario, P. (2000). On automatic identification of upper-limb movements using small-sized training sets of EMG signals. *Medical Engineering and Physics, 22*(8), 527–533.

Pandey, B., & Mishra, R. B. (2009). An integrated intelligent computing model for the interpretation of EMG based neuromuscular diseases. *Expert Systems with Applications, 36*(5), 9201–9213.

Park, S. H., & Lee, S. P. (1998). EMG pattern recognition based on artificial intelligence techniques. *IEEE Transactions on Rehabilitation Engineering, 6*(4).

Rafiee, J., Rafiee, M. A., Prause, N., & Schoen, M. P. (2009). Biorobotics: Optimized biosignal classification using mother wavelet matrix. In *IEEE 35th annual northeast bioengineering conference, harvard-MIT division of health sciences and technology, Cambridge, MA, USA, April 3–5, 2009*. doi:10.1109/NEBC.2009.4967645.

Rafiee, J., Rafiee, M. A., & Michaelsen, D. (2009). Female sexual responses using signal processing techniques. *The Journal of Sexual Medicine, 6*, 3086–3096.

Rafiee, J., & Tse, P. W. (2009). Use of autocorrelation of wavelet coefficients for fault diagnosis. *Mechanical Systems and Signal Processing, 23*, 1554–1572.

Rasheed, S., Stashuk, D. W., & Kamel, M. S. (2008). Diversity-based combination of non-parametric classifiers for EMG signal decomposition. *Pattern Analysis and Applications, 11*(3-4), 385–408.

Sebelius, F., Eriksson, L., Holmberg, H., Levinsson, A., Lundborg, G., Danielsen, N., et al. (2005). Classification of motor commands using a modified self-organising feature map. *Medical Engineering and Physics, 27*, 403–413.

Silvestro Micera, S., Sabatini, A. M., Dario, P., & Rossi, B. (1999). A hybrid approach to EMG pattern analysis for classification of arm movements using statistical and fuzzy techniques. *Medical Engineering and Physics, 21*, 303–311.

Subasi, A. (2005). Automatic recognition of alertness level from EEG by using neural network and wavelet coefficients. *Expert Systems with Applications, 28*(4), 701–711.

Subramani, P., Sahu, R., & Verma, S. (2006). Feature selection using Haar wavelet power spectrum. *BMC Bioinformatics*. art. no. 432.

Unser, M., & Aldroubi, A. (1996). A review of wavelets in biomedical applications. *Proceedings of the IEEE 84* (4), 626–638.

von Tscharner, V. (2000). Intensity analysis in time–frequency space of surface myoelectric signals by wavelets of specified resolution. *Journal of Electromyography and Kinesiology, 10*, 433–445.

von Tscharner, V. (2008). Spherical classification of wavelet transformed EMG intensity patterns. *Journal of Electromyography and Kinesiology*. doi:10.1016/j.jelekin.2008.07.001.

Vukova, T., Vydevska-Chichova, M., & Radicheva, N. (2008). Fatigue-induced changes in muscle fiber action potentials estimated by wavelet analysis. *Journal of Electromyography and Kinesiology, 18*, 397–409.

Xie, H.-B., Zheng, Y.-P., Guo, J.-Y., Chen, X., & Shi, J. (2009). Estimation of wrist angle from sonomyography using support vector machine and artificial neural network models. *Medical Engineering and Physics, 31*(3), 384–391.